

# Offline Signature Verification Using the Discrete Radon Transform and a Hidden Markov Model

**J. Coetzer**

*Department of Applied Mathematics, University of Stellenbosch, Matieland 7602, South Africa  
Email: jcoetzer@sun.ac.za*

**B. M. Herbst**

*Department of Applied Mathematics, University of Stellenbosch, Matieland 7602, South Africa  
Email: herbst@ibis.sun.ac.za*

**J. A. du Preez**

*Department of Electrical and Electronic Engineering, University of Stellenbosch, Matieland 7602, South Africa  
Email: dupreez@dsp.sun.ac.za*

*Received 31 October 2002; Revised 27 June 2003*

We developed a system that automatically authenticates offline handwritten signatures using the discrete Radon transform (DRT) and a hidden Markov model (HMM). Given the robustness of our algorithm and the fact that only global features are considered, satisfactory results are obtained. Using a database of 924 signatures from 22 writers, our system achieves an equal error rate (EER) of 18% when only high-quality forgeries (skilled forgeries) are considered and an EER of 4.5% in the case of only casual forgeries. These signatures were originally captured offline. Using another database of 4800 signatures from 51 writers, our system achieves an EER of 12.2% when only skilled forgeries are considered. These signatures were originally captured online and then digitally converted into static signature images. These results compare well with the results of other algorithms that consider only global features.

**Keywords and phrases:** offline signature verification, discrete Radon transform, hidden Markov model.

## 1. INTRODUCTION

The purpose of our research is to develop a system that automatically classifies handwritten signature images as authentic or fraudulent, with as little misclassifications as possible. At the same time, the processing requirements must be feasible so as to make the adoption of such an automated system economically viable.

Our work is inspired by, amongst others, the potential financial benefits that the automatic clearing of cheques will have for the banking industry. Despite an increasing number of electronic alternatives to paper cheques, fraud perpetrated at financial institutions in the United States has become a national epidemic. The National Check Fraud Center Report of 2000 [1] states that: "... cheque fraud and counterfeiting are among the fastest-growing crimes affecting the United States' financial system, producing estimated annual losses exceeding \$10 billion with the number continuing to rise at an alarming rate each year."

Since commercial banks pay little attention to verify-

ing signatures on cheques—mainly due to the number of cheques that are processed daily—a system capable of screening casual forgeries should already prove beneficial. In fact, most forged cheques contain forgeries of this type.

We developed a system that automatically authenticates documents based on the owner's handwritten signature. It should be noted that our system assumes that the signatures have already been extracted from the documents. Methods for extracting signature data from cheque backgrounds can be found in the following papers, [2, 3, 4]. Our system will assist commercial banks in the process of screening cheques and is not intended to replace the manual screening of cheques entirely. Those cheques of which the signatures do not sufficiently match a model of the owner's genuine signature are provisionally rejected. Generally, these rejected cheques will constitute a small percentage of the total number of cheques processed daily, and only these cheques are selected for manual screening.

Since the introduction of computers, modern society has become increasingly dependent on the electronic storage and

transmission of information. In many transactions, the electronic verification of a person's identity proved beneficial and this inspired the development of a wide range of automatic identification systems.

Plamondon and Srihari [5] note that automatic signature verification systems occupy a very specific niche among other automatic identification systems: "On the one hand, they differ from systems based on the possession of something (key, card, etc.) or the knowledge of something (passwords, personal information, etc.), because they rely on a specific, well learned gesture. On the other hand, they also differ from systems based on the biometric properties of an individual (finger prints, voice prints, retinal prints, etc.), because the signature is still the most socially and legally accepted means of personal identification."

Although handwritten signatures are by no means the most reliable means of personal identification, signature verification systems are inexpensive and nonintrusive. Handwritten signatures provide a direct link between the writer's identity and the transaction, and are therefore perfect for endorsing transactions.

A clear distinction should be made between signature verification systems and signature recognition systems. A signature *verification* system merely decides whether a claim that a particular signature belongs to a specific class (writer) is true or false. A signature *recognition* system, on the other hand, has to decide to which of a certain number of classes (writers) a particular signature belongs.

Diverse applications inspired researchers to investigate the feasibility of two distinct categories of automatic signature verification systems: those concerned with the verification of signature images and those concerned with the verification of signatures that were captured dynamically, using a special pen and digitising tablet. These systems are referred to as offline and online systems, respectively.

In *offline* systems, a signature is digitised using a handheld or flatbed scanner and only the completed writing is stored as an image. These images are referred to as *static* signatures. Offline systems are of interest in scenarios where only hard copies of signatures are available, for example where a large number of documents need to be authenticated.

In the *online* case, a special pen is used on an electronic surface such as a digitiser combined with a liquid crystal display. Apart from the two-dimensional coordinates of successive points of the writing, pen pressure as well as the angle and direction of the pen are captured dynamically and then stored as a function of time. The stored data is referred to as a *dynamic* signature and also contains information on pen velocity and acceleration. Online systems are of interest for "point-of-sale" and security applications.

Since online signatures also contain dynamic information, they are difficult to forge. It therefore comes as no surprise that offline signature verification systems are much less reliable than online systems.

A signature verification system typically focuses on the detection of one or more category of forged signatures. A *skilled* forgery is produced when the forger has unrestricted

access to one or more samples of the writer's actual signature (see Figure 1b). A *casual* forgery or a *simple* forgery (see Figure 1c) is produced when the forger is familiar with the writer's name, but does not have access to a sample of the actual signature—stylistic differences are therefore prevalent. A *random* forgery or *zero-effort* forgery (see Figure 1d) can be any random scribble or a signature of another writer, and may even include the forger's own signature. The genuine signatures and high quality forgeries for other writers are usually considered to be forgeries of this type.

Skilled forgeries can be subdivided into *amateur* and *professional* forgeries. A *professional forgery* is produced by an individual who has professional expertise in handwriting analysis. They are able to circumvent obvious problems and exploit their knowledge to produce high-quality, spacial forgeries (see Figure 2b).

In the context of online verification, amateur forgeries can be subdivided into *home-improved* and *over-the-shoulder* forgeries (see [6]). The category of home-improved forgeries contains forgeries that are produced when the forger has a paper copy of a genuine signature and has ample opportunity to practice the signature at home. Here the imitation is based only on the static image of the original signature (see Figure 2c). The category of over-the-shoulder forgeries contains forgeries that are produced immediately after the forger has witnessed a genuine signature being produced. The forger therefore learns not only the spatial image, but also the dynamic properties of the signature by observing the signing process (see Figure 2d). The different types of forgeries are summarised in Figure 3.

The features that are extracted from static signature images can be classified as global or local features. *Global features* describe an entire signature and include the discrete Wavelet transform [7], the Hough transform [8], horizontal and vertical projections [9], and smoothness features [10]. *Local features* are extracted at stroke and substroke levels and include unballistic motion and tremor information in stroke segments [11], stroke "elements" [9], local shape descriptors [12], and pressure and slant features [13].

Various pattern recognition *techniques* have been exploited to authenticate handwritten signatures (see Section 2). These techniques include template matching techniques [7, 9, 11], minimum distance classifiers [10, 12, 14, 15], neural networks [8, 13, 16], hidden Markov models (HMMs) [17, 18], and structural pattern recognition techniques.

Throughout this paper, the false rejection rate (FRR), the false acceptance rate (FAR), the equal error rate (EER), and the average error rate (AER) are used as quality performance measures. The FRR is the ratio of the number of genuine test signatures rejected to the total number of genuine test signatures submitted. The FAR is the ratio of the number of forgeries accepted to the total number of forgeries submitted. When the decision threshold is altered so as to decrease the FRR, the FAR will invariably increase, and vice versa. When a certain threshold is selected, the FRR is equal to the FAR. This error rate is called the EER and the corresponding threshold may be called the equal error threshold. The average of the FRR and FAR is called the AER. When a threshold is used,

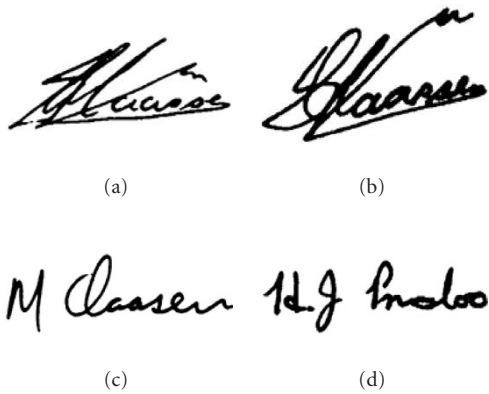


FIGURE 1: Example of a (a) genuine signature, (b) skilled forgery, (c) casual forgery, and (d) random forgery for the writer “M. Claasen.”

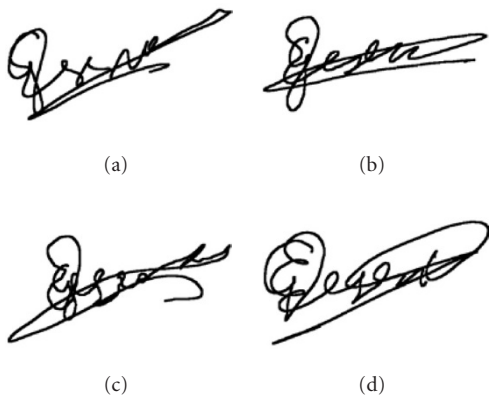


FIGURE 2: Example of a (a) genuine signature, (b) professional forgery, (c) home-improved forgery, and (d) over-the-shoulder forgery.

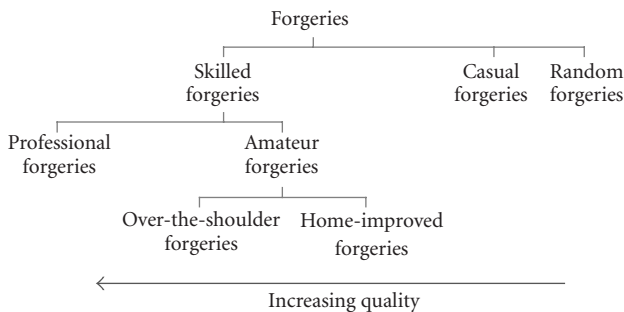


FIGURE 3: Types of forgeries.

that is, close to the equal error threshold, the FRR and FAR will not differ much. In this case the AER is approximately equal to the EER.

In this paper, we focus on offline signature verification. We are therefore not concerned with the verification of dy-

namic signatures nor with the recognition of signatures. Feature vectors are extracted from each static signature image by first calculating the discrete Radon transform (DRT). This is followed by further image processing. As we will explain in Section 3, the DRT is a very stable method of feature extraction. These features are global features since they are not extracted at stroke or substroke level. The DRT also enables us to construct an HMM, of which the states are organised in a ring, for each writer’s signature (see Section 4). Our verifier is constructed in such a way that it is geared towards the detection of only skilled and casual forgeries (see Section 5). We therefore do not consider random forgeries in this paper.

We test our system on two different data sets. We first test our system on our own independent database of static signatures. However, since it make sense to compare our results to those of another algorithm on the *same* database of signatures, and since offline signature databases are not freely available, we also test our system on a set of signatures that was originally captured online. Hans Dolging was kind enough to make this database available to us. Before we test our system on Dolging’s signatures, Dolging’s signatures are first transformed from dynamic signatures into static signature images (see Section 6.1). We then compare our results to the results of one of Dolging’s online algorithms. This algorithm uses an HMM and only considers the spacial coordinates of each writing. The results for both of these data sets are discussed in Section 6.3.

In Section 2, we describe a few *recent* offline signature verification systems. We categorise each of these systems according to the pattern recognition technique that is used. We also discuss the type of forgeries that each of these algorithms aim to detect, the type of features they exploit, whether the algorithm in question is geared towards the recognition or verification of signatures, the composition of each database, and the error rates for each algorithm. We then compare these approaches to ours. Our algorithm is discussed in detail in Sections 3, 4, 5, 6, 7, and 8.

## 2. OVERVIEW OF PRIOR WORK

A great deal of work has been done in the area of offline signature verification over the past two decades. A recent paper by Guo et al. [11] includes an extensive overview of previous work. Numerous methods and approaches are summarised in a number of survey articles. The state of the art from 1993 to 2000 is discussed in a paper by Plamondon and Srihari [5]. The period from 1989 to 1993 is covered by Leclerc and Plamondon [19] and the period before 1989 by Plamondon and Lorette [20]. Another survey was published by Sabourin et al. in 1992 [21]. A review of online signature verification by Gupta and McCabe in 1998 also includes a summary of some earlier work on the offline case [22].

Earlier work on offline signature verification deals primarily with casual and random forgeries. Many researchers therefore found it sufficient to consider only the global features of a signature.

As signature databases became larger and researchers moved toward more difficult skilled forgery detection tasks,

we saw a progression not only to more elaborate classifiers, but also to the increased use of local features and matching techniques.

We now briefly discuss some recent papers on offline signature verification.

#### *Template matching techniques*

Deng [7] developed a system that uses a closed contour tracing algorithm to represent the edges of each signature with several closed contours. The curvature data of the traced closed contours are decomposed into multiresolutional signals using wavelet transforms. The zero crossings corresponding to the curvature data are extracted as features for matching. A statistical measurement is devised to decide systematically which closed contours and their associated frequency data are most stable and discriminating. Based on these data, the optimal threshold value which controls the accuracy of the feature extraction process is calculated. Matching is done through dynamic time warping. Experiments are conducted independently on two data sets, one consisting of English signatures and the other consisting of Chinese signatures. For each experiment, twenty-five writers are used with ten training signatures, ten genuine test signatures, ten skilled forgeries, and ten casual forgeries per writer. When only the skilled forgeries are considered, AERs of 13.4% and 9.8% are reported for the respective data sets. When only the casual forgeries are considered, AERs of 2.8% and 3.0% are reported.

Fang [9] proposes two methods for the detection of skilled forgeries. These methods are evaluated on a database of 1320 genuine signatures from 55 writers and 1320 forgeries from 12 forgers. In determining the FRR, the leave-one-out method was adopted to maximise the use of the available genuine signatures. The *first method* calculates one-dimensional projection profiles for each signature in both the horizontal and vertical directions. These profiles are then optimally matched with reference profiles using dynamic programming. This method differs from previous methods in the sense that the distance between the warped projection profiles is not used in the decision. Instead, the positional distortion of each point of the sample profile, when warped onto a reference profile, is incorporated into a distance measure. A Mahalanobis distance is used instead of a simple Euclidean distance. The leave-one-out covariance (LOOC) method is adopted for this purpose, but the unreliable off-diagonal elements of the covariance matrices are set to zero. When binary and gray-scale signatures are considered, the best AERs for this method are 20.8% and 18.1%, respectively. The *second method* matches the individual stroke segments of a two-dimensional test signature directly with those of a template signature using a two-dimensional elastic matching algorithm. The objective of this algorithm is to achieve maximum similarity between the “elements” of a test signature and the “elements” of a reference signature, while minimising the deformation of these signatures. A gradient descent procedure is used for this purpose. Elements are short straight lines that approximate the skeleton of a signature. A

Mahalanobis distance with the same restrictions as for the first method is used. An AER of 23.4% is achieved for this method.

Guo [11] approached the offline problem by establishing a local correspondence between a model and a questioned signature. The questioned signature is segmented into consecutive stroke segments that are matched to the stroke segments of the model. The cost of the match is determined by comparing a set of geometric properties of the corresponding substrokes and computing a weighted sum of the property value differences. The least invariant features of the least invariant substrokes are given the largest weights, thus emphasizing features that are highly writer dependant. Using the local correspondence between the model and a questioned signature, the writer dependant information embedded at the substroke level is examined and unballistic motion and tremor information in each stroke segment are examined. Matching is done through dynamic time warping. A database with 10 writers is used with 5 training signatures, 5 genuine test signatures, 20 skilled forgeries, and ten casual forgeries per writer. An AER of 8.8% is obtained when only skilled forgeries are considered and an AER of 2.7% is obtained when only casual forgeries are considered.

#### *Minimum distance classifiers*

Fang [10] developed a system that is based on the assumption that the cursive segments of forged signatures are generally less smooth than that of genuine ones. Two approaches are proposed to extract the smoothness feature: a crossing method and a fractal dimension method. The smoothness feature is then combined with global shape features. Verification is based on a minimum distance classifier. An iterative leave-one-out method is used for training and for testing genuine test signatures. A database with 55 writers is used with 24 training signatures and 24 skilled forgeries per writer. An AER of 17.3% is obtained.

Fang [14] also developed a system that uses an elastic matching method to generate additional samples. A set of peripheral features, which is useful in describing both the internal and the external structures of signatures, is employed to represent a signature in the verification process. Verification is based on a Mahalanobis distance classifier. An iterative leave-one-out method is used for training and for testing genuine test signatures. The same database that was used in Fang’s previous paper [10] is again used here. The additional samples generated by this method reduced the AER from 15.6% to 11.4%.

Mizukami [15] proposed a system that is based on a displacement extraction method. The optimum displacement functions are extracted for any pair of signatures using minimization of a functional. The functional is defined as the sum of the squared Euclidean distance between two signatures and a penalty term that requires smoothness of the displacement function. A coarse-to-fine search method is applied to prevent the calculation from stopping at local minima. Based on the obtained displacement function, the

dissimilarity between the questioned signature and the corresponding authentic one is measured. A database with 20 writers is used with 10 training signatures, 10 genuine test signatures, and 10 skilled forgeries per writer. An AER of 24.9% is obtained.

Sabourin [12] uses granulometric size distributions for the definition of local shape descriptors in an attempt to characterise the amount of signal activity exciting each retina on the focus of an superimposed grid. He then uses a nearest neighbour and threshold-based classifier to detect random forgeries. A total error rate of 0.02% and 1.0% is reported for the respective classifiers. A database of 800 genuine signatures from 20 writers is used.

### Neural networks

Baltzakis [16] developed a neural network-based system for the detection of random forgeries. The system uses global features, grid features (pixel densities), and texture features (cooccurrence matrices) to represent each signature. For each one of these feature sets, a special two-stage perceptron one-class-one-network (OCON) classification structure is implemented. In the first stage, the classifier combines the decision results of the neural networks and the Euclidean distance obtained using the three feature sets. The results of the first stage classifier feed a second-stage radial basis function (RBF) neural network structure, which makes the final decision. A database is used which contains the signatures of 115 writers, with between 15 and 20 genuine signatures per writer. An average FRR and FAR of 3% and 9.8%, respectively is obtained.

Kaewkongka [8] uses the Hough transform (general Radon transform) to extract the parameterised Hough space from a signature skeleton as a unique characteristic feature of a signature. A backpropagation neural network is used to evaluate the performance of the method. The system is tested with 70 signatures from different writers and a recognition rate of 95.24% is achieved.

Quek [13] investigates the feasibility of using a pseudo-outer product-based fuzzy neural network for skilled forgery detection. He uses global baseline features (i.e., the vertical and horizontal position in the signature image which corresponds to the peak in the frequency histogram of the vertical and horizontal projection of the binary image, respectively), pressure features (that correspond to high pressure regions in the signature), and slant features (which are found by examining the neighbours of each pixel of the thinned signature). He then conducts two types of experiments. The first group of experiments use genuine signatures and forgeries as training data, while the second group of experiments use only genuine signatures as training data. These experiments are conducted on the signatures of 15 different writers, that is, 5 writers from 3 different ethnic groups. For each writer, 5 genuine signatures and 5 skilled forgeries are submitted. When genuine signatures and forgeries are used as training data, the average of the individual EERs is 22.4%. Comparable results are obtained when only genuine signatures are used as training data.

### Hidden Markov models

El-Yacoubi [17] uses HMMs and the cross-validation principle for random forgery detection. A grid is superimposed on each signature image, segmenting it into local square cells. From each cell, the pixel density is computed so that each pixel density represents a local feature. Each signature image is therefore represented by a sequence of feature vectors, where each feature vector represents the pixel densities associated with a column of cells. The cross-validation principle involves the use of a subset (validation set) of each writer's training set for validation purposes. Since this system aims to detect only random forgeries, subsets of other writers' training sets are used for impostor validation. Two experiments are conducted on two independent data sets, where each data set contains the signatures of 40 and 60 writers, respectively. Both experiments use 20 genuine signatures for training and 10 for validation. Both experiments use the forgeries of the first experiment for impostor validation. Each test signature is analyzed under several resolutions and the majority-vote rule is used to make a decision. AERs of 0.46% and 0.91% are reported for the respective data sets.

Justino [18] uses a discrete observation HMM to detect random, casual, and skilled forgeries. A grid segmentation scheme is used to extract three features: a pixel density feature, a pixel distribution feature (extended-shadow-code), and an axial slant feature. A cross-validation procedure is used to dynamically define the optimal number of states for each model (writer). Two data sets are used. The first data set contains the signatures of 40 writers with 40 genuine signatures per writer. This data set is used to determine the optimal codebook size for detecting random forgeries. This optimised system is then used to detect random, casual, and skilled forgeries in a second data set. The second data set contains the signatures of 60 writers with 40 training signatures, 10 genuine test signatures, 10 casual forgeries, and 10 skilled forgeries per writer. An FRR of 2.83% and an FAR of 1.44%, 2.50%, and 22.67% are reported for random, casual, and skilled forgeries, respectively.

### Comparison with our approach

Due to a lack of common signature databases, it is difficult to directly compare our system to the above systems. When comparing, we therefore first have to consider whether these systems are similar to our system or not. The rationale for this is that when a system is fundamentally very different from ours, it is very likely that a combination of this system and ours will result in a superior merged system. This will make their approach complementary to ours. Of all of these systems, three systems are probably the closest to ours.

Like our method, the first method by Fang [9] also considers one-dimensional projection profiles of each signature, but only in the horizontal and vertical directions. Their modelling *technique* however differs substantially from ours and is based on dynamic time warping. The positional distortion of each point of a sample profile, when warped onto a reference profile, is incorporated into a Mahalanobis distance measure. When only skilled forgeries are considered, their

system achieves a best AER of 20.8% for binary signatures. Our system achieves an EER of 17.7% when applied to our first database and an EER of 12.2% when applied to our second database.

The method by Kaewkongka [8] utilises the Hough transform, which is similar to the Radon transform, but is able to detect not only straight lines, but also other conical sections as well. Their modelling *technique* differs substantially from ours and is based on a backpropagation neural network. Their system is not a verification system though, and only aims to recognise signatures.

Like our method, the method by Justino [18] also utilises an HMM to detect casual and skilled forgeries. However, they use *features* that are very different from ours. A grid segmentation scheme is used to extract three features: a pixel density feature, a pixel distribution feature, and an axial slant feature. Although their system achieves better error rates than ours, the fact has to be taken into account that their system uses 40 training signatures per writer, while our system uses only 10 and 15 training signatures, respectively, when applied to our two data sets.

The approaches described in [12, 16, 17] use verifiers that are geared towards the detection of only *random* forgeries. The approaches described in [7, 10, 11, 12, 13, 14, 15, 16] utilise *techniques* that are fundamentally very different from ours, while the approaches described in [7, 10, 12, 14, 15, 16, 17] utilise *features* that are fundamentally very different from ours.

### 3. IMAGE PROCESSING

Each signature is scanned into a binary image at a resolution of 300 dots per inch, after which median filtering is applied to remove speckle noise. On average, a signature image has a width of 400 to 600 pixels and a height of 200 to 400 pixels. The image dimensions are not normalised.

Subsequently, the DRT of each signature is calculated. Each column of the DRT represents a projection or shadow of the signature at a certain angle. After these projections are processed and normalised, they represent a set of feature vectors (observation sequence) for the signature in question.

The DRT of an image is calculated as follows. Assume that each signature image consists of  $\Psi$  pixels in total, and that the intensity of the  $i$ th pixel is denoted by  $I_i$ ,  $i = 1, \dots, \Psi$ . The DRT is calculated using  $\beta$  nonoverlapping beams per angle and  $\Theta$  angles in total. The cumulative intensity of the pixels that lie within the  $j$ th beam is denoted by  $R_j$ ,  $j = 1, \dots, \beta\Theta$ . This is called the  $j$ th beam sum. In its discrete form, the Radon transform can therefore be expressed as follows:

$$R_j = \sum_{i=1}^{\Psi} w_{ij} I_i, \quad j = 1, 2, \dots, \beta\Theta, \quad (1)$$

where  $w_{ij}$  indicates the contribution of the  $i$ th pixel to the  $j$ th beam sum (see Figure 4). The value of  $w_{ij}$  is found through two-dimensional interpolation. Each projection therefore contains the beam sums that are calculated at a given angle.

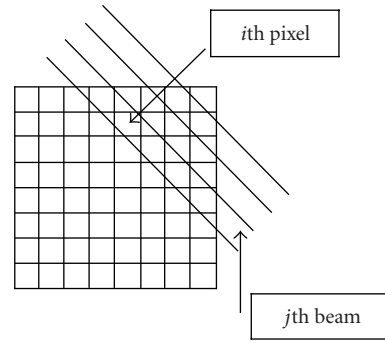


FIGURE 4: Discrete model for the Radon transform with  $w_{ij} \approx 0.9$ .

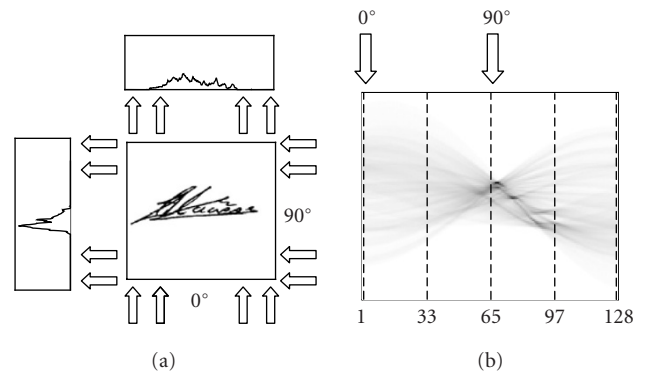


FIGURE 5: (a) A signature and its projections calculated at angles of  $0^\circ$  and  $90^\circ$ . (b) The DRT displayed as a gray-scale image. This image has  $\Theta = 128$  columns, where each column represents a projection.

The accuracy of the DRT is determined by  $\Theta$  (the number of angles),  $\beta$  (the number of beams per angle), and the accuracy of the interpolation method.

Note that the continuous form of the Radon transform can be inverted through analytical means. The DRT therefore contains almost the same information as the original image and can be efficiently calculated with an algorithm by Bracewell [23].

Our system calculates the DRT at  $\Theta$  angles. These angles are equally distributed between  $0^\circ$  and  $180^\circ$ . A typical signature and its DRT are shown in Figure 5. The dimension of each projection is subsequently altered from  $\beta$  to  $d$ . This is done by first decimating all the zero-valued components from each projection. These decimated vectors are then shrunk or expanded to a length of  $d$  through interpolation. Although almost all the information in the original signature image is contained in the projections at angles that range from  $0^\circ$  to  $180^\circ$ , the projections at angles that range from  $180^\circ$  to  $360^\circ$  are also included in the observation sequence. These additional projections are added to the observation sequence in order to ensure that the sequence fits the topology of our HMM (see Section 4.2). Since these projections are simply reflections of the projections already calculated, no additional calculations are necessary. An observation sequence therefore consists of  $T = 2\Theta$  feature vectors, that

is,  $X_1^T = \{x_1, x_2, \dots, x_T\}$ . Each vector is subsequently normalised by the variance of the intensity of the entire set of  $T$  feature vectors. Each signature pattern is therefore represented by an observation sequence that consists of  $T$  observations, where each observation is a feature vector of dimension  $d$ . The experimental results and computational requirements for various values of  $d$  and  $\Theta$  are discussed in Sections 6 and 7, respectively.

The DRT, as a feature extraction technique, has several *advantages*. Although the DRT is not a shift invariant representation of a signature image, shift and scale invariance is ensured by the subsequent image processing. Each signature is a static image and contains no dynamic information. Since the feature vectors are obtained by calculating projections at different angles, simulated time evolution is created from one feature vector to the next, where the angle is the dynamic variable. This enables us to construct an HMM for each signature (see Section 4). The DRT is calculated at angles that range from  $0^\circ$  to  $360^\circ$  and each observation sequence is then modelled by an HMM of which the states are organised in a ring (see Section 4.2). This ensures that each set of feature vectors is rotation invariant. Our system is also robust with respect to moderate levels of noise. These advantages are now discussed in more detail.

#### Noise

We explained earlier in this section that the zero-valued components of each projection are decimated before the remaining non-zero components are shrunk or expanded through interpolation. In this way, a feature vector with the required dimension is obtained. The decimation of the zero-valued components ensures that moderate levels of noise (which are represented by a few additional small-valued components within certain projections) are “attached” to the other non-zero components before the decimated vector is shrunk or expanded. Since the dimension of the feature vectors are high compared to the number of these additional components, the incorporation of these components has little effect on the overall performance of the system.

#### Shift invariance

Although the DRT is not a shift invariant representation of a signature image, shift invariance is ensured by the subsequent image processing. The zero-valued components of each projection are decimated and the corresponding feature vector is constructed from the remaining components only.

#### Rotation invariance

The DRT is calculated at angles that range from  $0^\circ$  to  $360^\circ$  and each set of feature vectors is then modelled by an HMM of which the states are organised in a ring (see Section 4.2). Each signature is therefore represented by a set of feature vectors that is rotation invariant.

#### Scale invariance

For each projection, scale invariance has to be achieved in the direction perpendicular to the direction in which the image

is scanned, that is, perpendicular to the beams, and in the direction parallel to the beams. Scale invariance perpendicular to the beams is ensured by shrinking or expanding each decimated projection to the required dimension. Scale invariance parallel to the beams is achieved by normalizing the intensity of each feature vector. This is achieved by dividing each feature vector by the variance of the intensity of the entire set of feature vectors.

## 4. SIGNATURE MODELLING

We use a first-order continuous observation HMM to model each writer’s signature. For a tutorial on HMMs, the reader is referred to a paper by Rabiner [24] and the book by Deller et al. [25].

### 4.1. Notation

We use the following notation for an HMM  $\lambda$ .

- (1) We denote the  $N$  individual states as

$$S = \{s_1, s_2, \dots, s_N\} \quad (2)$$

and the state at time  $t$  as  $q_t$ .

- (2) The initial state distribution is denoted by  $\pi = \{\pi_i\}$ , where

$$\pi_i = P(q_1 = s_i), \quad i = 1, \dots, N. \quad (3)$$

- (3) The state transition probability distribution is denoted by  $A = \{a_{i,j}\}$ , where

$$a_{i,j} = P(q_{t+1} = s_j \mid q_t = s_i), \quad i = 1, \dots, N, \quad j = 1, \dots, N. \quad (4)$$

- (4) The probability density function (pdf), which quantifies the similarity between a feature vector  $x$  and the state  $s_j$ , is denoted by

$$f(x|s_j, \lambda), \quad j = 1, \dots, N. \quad (5)$$

### 4.2. HMM topology

We use an HMM, the states of which are organised in a ring (see Figure 6). Our model is equivalent to a left-to-right model, but a transition from the last state to the first state is allowed. Since the HMM is constructed in such a way that it is equally likely to enter the model at any state, and the feature vectors are obtained from all the projections, that is, the projections calculated at angles ranging from  $0^\circ$  to  $360^\circ$ , the ring topology of our HMM guarantees that the signatures are rotation invariant. Each state in the HMM represents one or more feature vectors that occupy similar positions in a  $d$ -dimensional feature space. This implies that the HMM groups certain projections (columns of the DRT) together. It is important to note that this segmentation process only takes place after some *further* image processing has been conducted on the original projections.

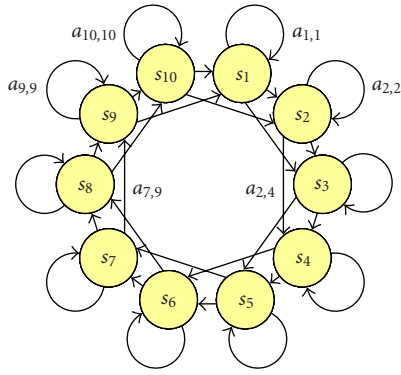


FIGURE 6: An example of an HMM with a ring topology. This model has ten states with one state skip.

### 4.3. Training

Each model is trained using the Viterbi reestimation technique. The dissimilarity between an observation sequence  $X$  and a model  $\lambda$  can therefore be calculated as follows (see [24]):

$$d(X, \lambda) = -\ln(f(X|\lambda)). \quad (6)$$

In real-world scenarios, each writer can only submit a small number of training samples when he or she is enrolled into the system. Since our algorithm uses feature vectors with a high dimension, the reestimated covariance matrix of the pdf for each state is not reliable and may even be singular. A Mahalanobis distance measure can therefore not be found. Consequently, these covariance matrices are not reestimated and are initially set to  $0.5I$ , where  $I$  is the identity matrix. Only the mean vectors are reestimated, which implies that the dissimilarity values are based on an Euclidean distance measure.

We assume that training signatures, genuine test signatures, and forgeries are available for only a limited number of writers, that is, for those writers in our database. No forgeries are used in the training process since our system aims to detect only skilled and casual forgeries, and these type of forgeries are not available when our system is implemented. The genuine test signatures and forgeries are used to determine the error rates for our system (see Section 6). Assuming that there are  $W$  writers in our database, the training signatures for each writer are used to construct an HMM, resulting in  $W$  models, that is  $\{\lambda_1, \lambda_2, \dots, \lambda_W\}$ .

When the training set for writer  $w$  is denoted by  $\{X_1^{(w)}, X_2^{(w)}, \dots, X_{N_w}^{(w)}\}$ , where  $N_w$  is the number of samples in the training set, the dissimilarity between every training sample and the model is used to determine the following statistics for the writer's signature:

$$\begin{aligned} \mu_w &= \frac{1}{N_w} \sum_{i=1}^{N_w} d(X_i^{(w)}, \lambda_w), \\ \sigma_w^2 &= \frac{1}{N_w - 1} \sum_{i=1}^{N_w} (d(X_i^{(w)}, \lambda_w) - \mu_w)^2. \end{aligned} \quad (7)$$

## 5. VERIFICATION

When a system aims to detect only random forgeries, subsets of other writers' training sets can be used to model "typical" forgeries. This is called "impostor validation" and can be achieved through strategies like test normalization (see [26]). These techniques enable one to construct verifiers that detect random forgeries very accurately (see [12, 17]). Since we aim to detect only skilled and casual forgeries, and since models for these forgeries are generally unobtainable, we are not able to utilise any of these impostor validation techniques. We also do not use any subset of genuine signatures for validation purposes.

Our verifier is constructed as follows. When a claim is made that the test pattern  $X_{\text{Test}}^{(w)}$  belongs to writer  $w$ , the pattern is first matched with the model  $\lambda_w$  through Viterbi alignment. This match is quantified by  $f(X_{\text{Test}}^{(w)}|\lambda_w)$ . The dissimilarity between the test pattern and the model is then calculated as follows (see [24]):

$$d(X_{\text{Test}}^{(w)}, \lambda_w) = -\ln(f(X_{\text{Test}}^{(w)}|\lambda_w)). \quad (8)$$

In order to use a global threshold for all writers, Dolfling [6] suggests that every dissimilarity value in (8) is normalised, using the statistics of the claimed writer's signature, that is, (7):

$$d_{\text{Mah}}(X_{\text{Test}}^{(w)}, \lambda_w) = \frac{d(X_{\text{Test}}^{(w)}, \lambda_w) - \mu_w}{\sigma_w}, \quad (9)$$

where  $d_{\text{Mah}}(X_{\text{Test}}^{(w)}, \lambda_w)$  denotes the normalised dissimilarity between the test pattern and the model of the claimed writer's signature. This normalization is based on the assumption that the dissimilarity value in (8) is based on a Mahalanobis distance measure.

When only the mean vectors are reestimated though, the dissimilarity value in (8) is based on an Euclidean distance measure. When this is the case, we found that significantly better results are obtained when the standard deviation of the dissimilarities of the training set, that is,  $\sigma_w$  in (9), is replaced by the mean  $\mu_w$ , that is,

$$d_{\text{Eucl}}(X_{\text{Test}}^{(w)}, \lambda_w) = \frac{d(X_{\text{Test}}^{(w)}, \lambda_w) - \mu_w}{\mu_w}. \quad (10)$$

A sliding threshold  $\tau$ , where  $\tau \in (-\infty, \infty)$ , is used to determine the error rates for the test patterns. When  $d_{\text{Eucl}}(X_{\text{Test}}^{(w)}, \lambda_w) < \tau$ , that is,

$$d(X_{\text{Test}}^{(w)}, \lambda_w) < \mu_w(1 + \tau), \quad (11)$$

the claim is accepted, otherwise, the claim is rejected. When  $\tau = 0$ , all the test patterns for which  $d(X_{\text{Test}}^{(w)}, \lambda_w) \geq \mu_w$  are rejected. This almost always results in an FRR close to 100% and an FAR close to 0%. When  $\tau \rightarrow \infty$ , all the test patterns for which  $d(X_{\text{Test}}^{(w)}, \lambda_w)$  is finite are accepted. This always results in an FRR of 0% and an FAR of 100%.



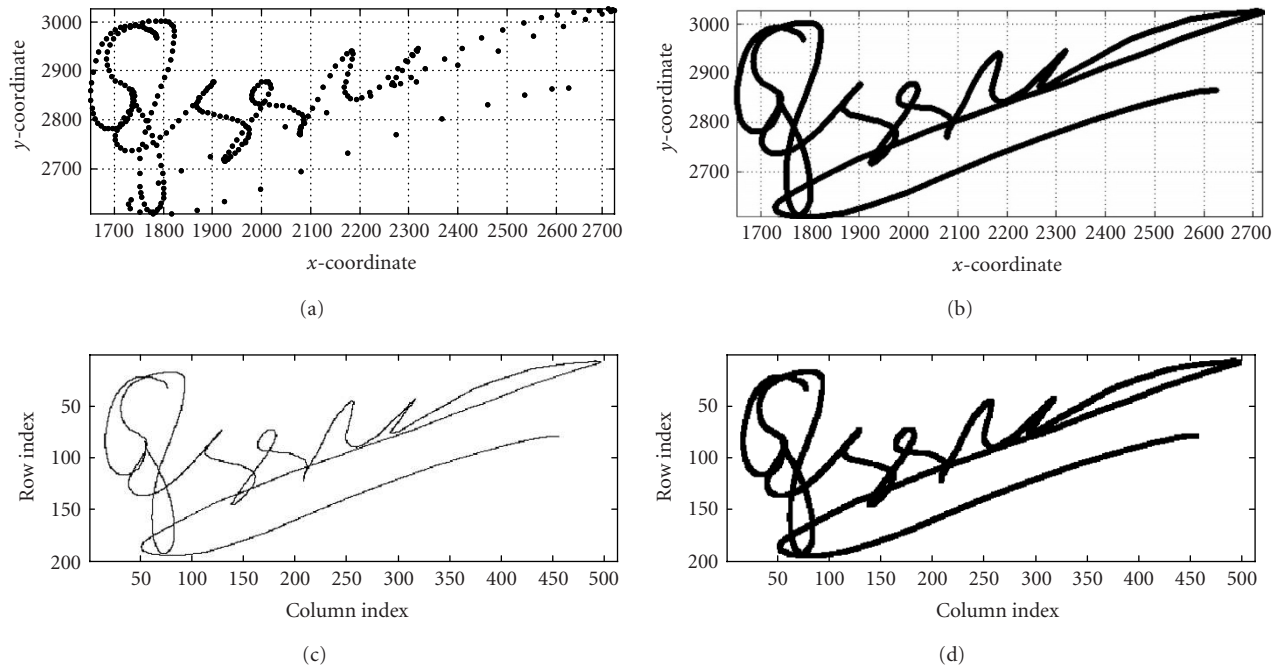


FIGURE 7: Conversion of dynamic signature data into a static signature image. (a) The “pen-down” coordinates of a signature that was captured online. (b) One hundred interpolatory points are inserted between each two successive coordinate pairs. (c) A signature image with a stroke width of one. (d) A signature image with a stroke width of five.

## 6. EXPERIMENTS

Experiments are conducted on two different data sets. The first data set, we call it the Stellenbosch data set, consists of signature images that were captured offline from designated areas on blank sheets of paper. The second data set, we call it Dolfig’s data set, consists of dynamic signatures that were originally captured for Hans Dolfig’s Ph.D. thesis [6]. We use the pen-tip coordinates to convert each dynamic signature into an “ideal” signature image, that is, a signature that contains no background noise and has a uniform stroke width.

### 6.1. Data

#### *The Stellenbosch data set*

Our first data set contains 924 signatures from 22 writers. Ten training signatures were obtained from each writer during an initial enrollment session. Thirty-two test signatures, that consists of 20 genuine signatures, 6 skilled forgeries, and 6 casual forgeries, were subsequently obtained over a period of two weeks. The 20 genuine test signatures consist of two sets of 10 signatures each. These signatures were supplied by the same writers one week and two weeks after the enrollment session. The forgeries were obtained from 6 forgers. The casual forgeries were obtained first. Only the name of the writer was supplied to the forgers and they did not have access to the writer’s signatures. The skilled forgeries were then obtained from the same group of forgers. They were provided with several samples of each writer’s genuine signature and

were allowed ample opportunity to practice. Each forger submitted 1 casual forgery and 1 skilled forgery for each writer. The writers were instructed to produce each signature within an appropriate rectangular region on a white sheet of paper. The signatures were then digitised with a flatbed scanner at a resolution of 300 dots per inch. The genuine signatures were produced with different pens and the forgeries were produced with the same pens that were used for producing the genuine signatures. These signatures are free of excessive noise, smears, and scratches.

#### *Dolfig’s data set*

We also test our system on a second data set. Since offline signature databases are not freely available, we use a set of signatures that were originally captured online. We then convert these online signatures into static signature images. Since Hans Dolfig used this data set to evaluate one of his online algorithms (see [6]), we are able to compare his results to ours. Dolfig’s data set contains 4800 signatures from 51 writers and differs from the Stellenbosch data set in the sense that the signatures were originally captured online for Hans Dolfig’s Ph.D. thesis [6]. Each of these signatures contains static *and* dynamic information captured at 160 sample points per second. Each of these sample points contains information on pen-tip position, pen pressure, and pen tilt. Static signature images are constructed from this data using only the pen-tip position, that is, the  $x$  and  $y$  coordinates, for those sample points for which the pen pressure is nonzero (see Figure 7a). These signature images are therefore “ideal”

TABLE 1: Data sets.

| Data set | Data acquisition method | Number of writers | Training signatures per writer | Genuine test signatures | Number of forgeries |                 |              |
|----------|-------------------------|-------------------|--------------------------------|-------------------------|---------------------|-----------------|--------------|
|          |                         |                   |                                |                         | Skilled             | Casual          | Random       |
| S'bosch  | Offline                 | 22                | 10                             | 440                     | 132                 | 132             | 19 404       |
| Dolfing  | Online                  | 51                | 15                             | 765                     | Professional<br>270 | Amateur<br>3000 | —<br>240 000 |

in the sense that they contain virtually no background noise. This acquisition method also ensures a uniform stroke width within each signature and throughout the data set. One hundred interpolatory points are inserted between each two successive coordinate pairs. Linear interpolation is used for this purpose and only those coordinate pairs that form part of the same “pen-down” segment are connected in this way (see Figure 7b). These coordinates are then rescaled in such a way that the range of the coordinate with the greater range is normalised to roughly 480, while the spatial aspect ratio of the entire signature is maintained. An image that consists of only zeros and of which the larger dimension is 512 is subsequently constructed. The normalised coordinates are then translated and rounded to the nearest integer so that the superimposed coordinates are roughly in the middle of the image. The pixel coordinates which coincide with these superimposed coordinates are then set to one. The resulting signature image has a stroke width of one (see Figure 7c). In order to obtain signatures with a stroke width of five, each signature is dilated using a square morphological mask of dimension five (see Figure 7d).

Dolfing's data set contains four types of forgeries: random forgeries, over-the-shoulder forgeries, home-improved forgeries, and professional forgeries (see Section 1). A summary of the two data sets is given in Table 1.

## 6.2. Experimental setup

### The Stellenbosch data set

We consider 30 genuine signatures, 6 skilled forgeries, and 6 casual forgeries for each writer. For each writer, 10 genuine signatures are used for training and 20 for testing. No genuine signatures are used for validation purposes.

### Dolfing's data set

We consider 30 genuine signatures for each writer, an average of 58.8 amateur forgeries per writer, and an average of 5.3 professional forgeries per writer. For each writer, 15 genuine signatures are used for training and 15 for testing. No genuine signatures are used for validation purposes.

## 6.3. Results

### The Stellenbosch data set

Let  $\ell$  denote the number of allotted forward links in our HMM. Figure 8 shows the FRR and FAR as functions of our threshold parameter  $\tau \in [-0.1, 1]$ , when  $d = 512$ ,  $\Theta = 128$ ,  $N = 64$ , and  $\ell = 1$ . The FRR, the FAR for a test set that

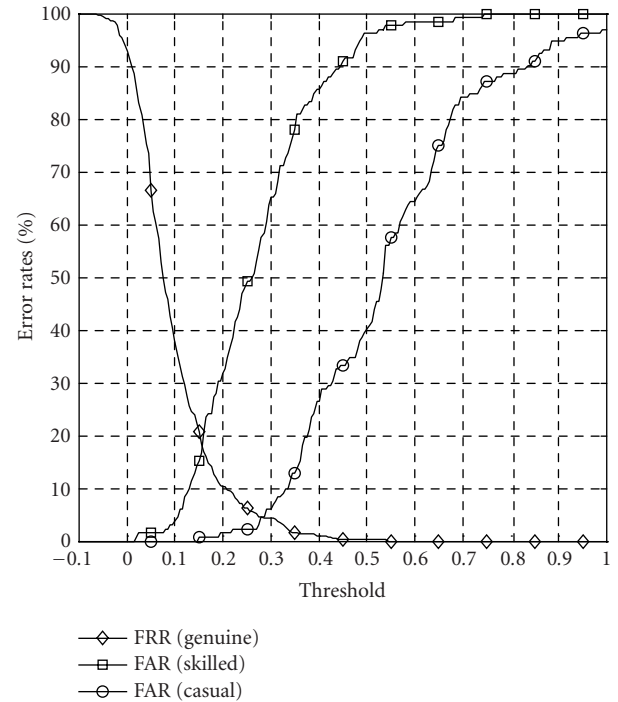


FIGURE 8: The Stellenbosch data set. Graphs for the FRR and the FAR when  $d = 512$ ,  $\Theta = 128$ ,  $N = 64$ , and  $\ell = 1$ .

contains only skilled forgeries, and the FAR for a test set that contains only casual forgeries are plotted on the same system of axes. When, for example, a threshold of  $\tau = 0.16$  is selected, equation (11) implies that all the test patterns for which  $d(X_{\text{Test}}^{(w)}, \lambda_w) \geq 1.16\mu_w$  are rejected—the other patterns are accepted. When only skilled forgeries are considered, this threshold selection will ensure an EER of approximately 18%. When only casual forgeries are considered, our algorithm achieves an EER of 4.5%.

Table 2 tabulates the EER as well as a local FRR and FAR, for various values of  $d$ ,  $\Theta$ ,  $N$ , and  $\ell$ . It is clear that when the dimension of the feature vectors is decreased from  $d = 512$  to  $d = 256$  or even to  $d = 128$ , the performance of the system is not significantly compromised. The performance of our system is generally enhanced when the number of feature vectors, that is,  $T = 2\theta$ , or the number of states in the HMM, that is,  $N$ , is increased. The best results are obtained when only one forward link is allowed in the HMM, that is, when  $\ell = 1$ .

TABLE 2: The Stellenbosch data set: summary of results.

| $d$               | $\Theta$ | $N$ | $\ell$ | FRR (%) | FAR (%) | EER (%)     |
|-------------------|----------|-----|--------|---------|---------|-------------|
| <b>512</b>        | 128      | 64  | 1      |         |         |             |
| Skilled forgeries |          |     |        | 10.2    | 25.4    | <b>17.9</b> |
| Casual forgeries  |          |     |        | 0.2     | 32.6    | <b>4.5</b>  |
| 512               | 128      | 64  | 2      |         |         |             |
| Skilled forgeries |          |     |        | 10.2    | 25.7    | 18.5        |
| Casual forgeries  |          |     |        | 0.2     | 34.1    | 4.6         |
| 512               | 128      | 64  | 4      |         |         |             |
| Skilled forgeries |          |     |        | 10.2    | 25.9    | 18.2        |
| Casual forgeries  |          |     |        | 0.2     | 35.6    | 4.6         |
| 512               | 128      | 32  | 1      |         |         |             |
| Skilled forgeries |          |     |        | 10.2    | 25.5    | 19.2        |
| Casual forgeries  |          |     |        | 0.2     | 34.8    | 5.4         |
| 512               | 128      | 16  | 1      |         |         |             |
| Skilled forgeries |          |     |        | 10.2    | 32.1    | 20.7        |
| Casual forgeries  |          |     |        | 0.2     | 43.1    | 6.2         |
| <b>256</b>        | 128      | 64  | 1      |         |         |             |
| Skilled forgeries |          |     |        | 10.2    | 25.3    | <b>17.7</b> |
| Casual forgeries  |          |     |        | 0.2     | 32.6    | <b>4.5</b>  |
| 256               | 128      | 32  | 1      |         |         |             |
| Skilled forgeries |          |     |        | 10.2    | 26.4    | 19.4        |
| Casual forgeries  |          |     |        | 0.2     | 35.6    | 5.4         |
| 256               | 64       | 32  | 1      |         |         |             |
| Skilled forgeries |          |     |        | 10.2    | 25.4    | 18.4        |
| Casual forgeries  |          |     |        | 0.2     | 34.8    | 5.3         |
| <b>128</b>        | 64       | 32  | 1      |         |         |             |
| Skilled forgeries |          |     |        | 10.2    | 24.6    | <b>18.3</b> |
| Casual forgeries  |          |     |        | 0.2     | 34.8    | <b>5.4</b>  |
| 128               | 32       | 16  | 1      |         |         |             |
| Skilled forgeries |          |     |        | 0.2     | 38.7    | 22.0        |
| Casual forgeries  |          |     |        | 0.2     | 48.4    | 6.2         |

### Dolfing's data set

The results of our algorithm is compared to the results of an algorithm that was developed by Hans Dolfing for his Ph. D. thesis [6].

Dolfing developed HMM-based algorithms for the verification and recognition of dynamic signatures. Since our algorithm is suited for the verification of static signatures, that is, signature images, we compare our results to the results of Dolfing's algorithm that only considers the spatial coordinates of each dynamic signature. It is important to note that, in order to construct an HMM for each writer's signature, Dolfing's algorithm also uses the sequence in which these spacial coordinates were produced. Our algorithm is therefore at a disadvantage since it has no knowledge of the stroke sequence, and simulated time evolution had to be created by taking the DRT of each signature image.

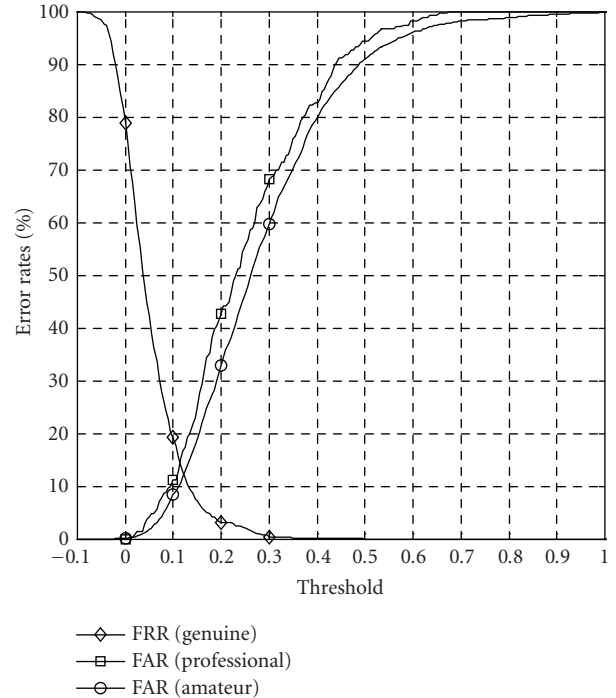


FIGURE 9: Dolfing's data set. Graphs for the FRR and the FAR when  $d = 512$ ,  $\Theta = 128$ ,  $N = 64$ , and  $\ell = 1$ .

TABLE 3: Dolfing's data set: summary of results.

| EER (%) | Amateur forgeries   |               |
|---------|---------------------|---------------|
|         | Dolfing's algorithm | Our algorithm |
|         | 13.3                | 12.2          |

Figure 9 shows the FRR and FAR as functions of our threshold parameter  $\tau \in [-0.1, 1]$ , when  $d = 512$ ,  $\Theta = 128$ ,  $N = 64$ , and  $\ell = 1$ . The FRR, the FAR for a test set that contains only professional forgeries, and the FAR for a test set that contains only amateur forgeries are plotted on the same system of axes. The error rates for Dolfing's algorithm, when applied to only professional forgeries, were not published. For illustrational purposes however, we include our FAR for only professional forgeries in Figure 9. When only amateur forgeries are considered, our algorithm achieves an EER of 12.2%. These results compare well with the results for Dolfing's algorithm. Dolfing's algorithm (see [6, page 160]) achieves an EER of 13.3%. These results are tabulated in Table 3.

## 7. COMPUTATIONAL REQUIREMENTS

An automatic signature verification system can only be economically viable when the processing requirements are feasible. The practicality of our system as a real-time application depends on the number of floating point operations (flops) required to verify a test signature. The bulk of these flops are

required to calculate the DRT. Much less flops are required to match a set of feature vectors (which represents a test signature) with the HMM of the claimed writer's signature.

### DRT

We assume that the original image consists of  $\Psi$  pixels and that  $\Theta$  angles (between  $0^\circ$  and  $180^\circ$ ) are used to calculate the DRT. When  $\beta$  (i.e., the number of beams per angle) is taken to be equal to the highest dimension of the original image, the number of flops required to calculate the DRT is on the order of  $4\Psi\Theta$  (see [23]). This implies that for an average image of  $500 \times 300$  pixels, with  $\Theta = 128$  and  $\beta = 500$ , the number of flops required to calculate the DRT is on the order of  $76.8 \times 10^6$ . With these parameters, an EER of 17.9% is achieved when only skilled forgeries from the Stellenbosch data set are considered. However, these computational requirements can be significantly reduced without compromising the performance of our system (see Table 2). The number of flops required to calculate the DRT of an image of  $256 \times 128$  pixels, with  $\Theta = 64$  and  $\beta = 256$ , is on the order of  $8.4 \times 10^6$ . With these parameters, an EER of 18.4% is achieved when only skilled forgeries from the Stellenbosch data set are considered.

### Matching

Since the states in our HMM are organised in a ring and the dissimilarity value in (8) is based on an Euclidean distance measure, the number of flops required to match an observation sequence with an HMM is on the order of  $T(N\ell + d)$ . Therefore, despite the high dimensionality of the feature vectors, relatively few flops are required to match an observation sequence with an HMM. With  $d = 512$ ,  $T = 256$ ,  $N = 64$ , and  $\ell = 1$ , on the order of only 147 456 flops are required. With these parameters, an EER of 17.9% is achieved when only skilled forgeries from the Stellenbosch data set are considered. With  $d = 256$ ,  $T = 128$ ,  $N = 32$  and  $\ell = 1$ , on the order of only 36 864 flops are required. With these parameters, an EER of 18.4% is achieved when only skilled forgeries from the Stellenbosch data set are considered (see Table 2).

## 8. DISCUSSION, CONCLUSIONS, AND FUTURE WORK

The DRT is a stable and robust method of feature extraction. The DRT creates simulated time evolution from one feature vector to the next and enables us to model a signature with an HMM. Our system is not sensitive to moderate levels of noise, and the feature vectors are extracted in such a way that rotation, shift, and scale invariance is ensured.

Given the robustness of our algorithm and the fact that only global features are considered, satisfactory results are obtained when our algorithm is applied to an independent database (see Section 6.1) of 924 signatures from 22 writers. These results compare well with the results for other systems that only consider global features (see Sections 2 and 6.3).

When our algorithm is applied to Hans Dolfig's database of dynamic signatures (see Section 6.1), our results compare well with an algorithm by Dolfig that only con-

siders the spatial coordinates of each dynamic signature (see Section 6.3). This is despite the fact that our algorithm only considers a static image of each signature, while Dolfig's algorithm has knowledge of the sequence in which the spatial coordinates were produced. Dolfig's database consists of 4800 signatures from 51 writers.

Our system uses only global features. However, most recent systems also utilise local features for verification purposes, that is, features at stroke and substroke levels, and their feature extraction techniques require extensive preprocessing (see Section 2). Our system does not outperform all of these systems. These systems do however utilise either a technique or features that are fundamentally very different from ours. This implies that it is very likely that a combination of their systems and ours will result in a superior merged system, making their approaches complementary to ours. We also expect a significant improvement in our results when local features are incorporated into our algorithm. This is currently being investigated.

## REFERENCES

- [1] National Check Fraud Center, *National Check Fraud Center Report*, 2000.
- [2] S. Djeziri, F. Nouboud, and R. Plamondon, "Extraction of signatures from cheque background based on a filiformity criterion," *IEEE Trans. Image Processing*, vol. 7, no. 10, pp. 1425–1438, 1998.
- [3] A. L. Koerich and L. L. Lee, "Automatic extraction of filled-in information from bankchecks based on prior knowledge about layout structure," in *Advances in Document Image Analysis: First Brazilian Symposium*, vol. 1339 of *Lecture Notes in Computer Science*, pp. 322–333, Curitiba, Brazil, November 1997.
- [4] J. E. B. Santos, E. Bortolozzi, and R. Sabourin, "A simple methodology to bankcheck segmentation," in *Advances in Document Image Analysis: First Brazilian Symposium*, vol. 1339 of *Lecture Notes in Computer Science*, pp. 334–343, Curitiba, Brazil, November 1997.
- [5] R. Plamondon and S. N. Srihari, "On-line and off-line handwriting recognition: a comprehensive survey," *IEEE Trans. on Pattern Analysis and Machine Intelligence*, vol. 22, no. 1, pp. 63–84, 2000.
- [6] J. G. A. Dolfig, *Handwriting recognition and verification. A hidden Markov approach*, Ph.D. thesis, Eindhoven University of Technology, 1998.
- [7] P. S. Deng, H. Y. M. Liao, C.-W. Ho, and H.-R. Tyan, "Wavelet-based off-line handwritten signature verification," *Computer Vision and Image Understanding*, vol. 76, no. 3, pp. 173–190, 1999.
- [8] T. Kaewkongka, K. Chamnongthai, and B. Thipakorn, "Off-line signature recognition using parameterized hough transform," in *Proc. 5th International Symposium on Signal Processing and Its Applications*, pp. 451–454, Brisbane, Australia, 1999.
- [9] B. Fang, C. H. Leung, Y. Y. Tang, K. W. Tse, P. C. K. Kwok, and Y. K. Wong, "Off-line signature verification by the tracking of feature and stroke positions," *Pattern Recognition*, vol. 36, pp. 91–101, 2003.
- [10] B. Fang, Y. Y. Wang, C. H. Leung, et al., "Offline signature verification by the analysis of cursive strokes," *International Journal of Pattern Recognition and Artificial Intelligence*, vol. 15, no. 4, pp. 659–673, 2001.

- [11] J. K. Guo, D. Doermann, and A. Rosenfeld, "Forgery detection by local correspondence," *International Journal of Pattern Recognition and Artificial Intelligence*, vol. 15, no. 4, pp. 579–641, 2001.
- [12] R. Sabourin, G. Genest, and F. Prêteux, "Off-line signature verification by local granulometric size distributions," *IEEE Trans. on Pattern Analysis and Machine Intelligence*, vol. 19, no. 9, pp. 976–988, 1997.
- [13] C. Quek and R. W. Zhou, "Antiforgery: a novel pseudo-outer product based fuzzy neural network driven signature verification system," *Pattern Recognition Letters*, vol. 23, no. 14, pp. 1795–1816, 2002.
- [14] B. Fang, C. H. Leung, Y. Y. Tang, P. C. K. Kwok, K. W. Tse, and Y. K. Wong, "Off-line signature verification with generated training samples," *IEE Proceedings - Vision, Image and Signal Processing*, vol. 149, no. 2, pp. 85–90, 2002.
- [15] Y. Mizukami, M. Yoshimura, H. Miike, and I. Yoshimura, "An off-line signature verification system using an extracted displacement function," *Pattern Recognition Letters*, vol. 23, no. 13, pp. 1569–1577, 2002.
- [16] H. Baltzakis and N. Papamarkos, "A new signature verification technique based on a two-stage neural network classifier," *Engineering Applications of Artificial Intelligence*, vol. 14, pp. 95–103, 2001.
- [17] A. El-Yacoubi, E. J. R. Justino, R. Sabourin, and F. Bortolozzi, "Off-line signature verification using HMMs and cross-validation," in *IEEE International Workshop on Neural Networks for Signal Processing*, pp. 859–868, Sydney, Australia, December 2000.
- [18] E. J. R. Justino, F. Bortolozzi, and R. Sabourin, "Off-line signature verification using HMM for random, simple and skilled forgeries," in *International Conference on Document Analysis and Recognition*, vol. 1, pp. 105–110, Seattle, Wash, USA, 2001.
- [19] F. Leclerc and R. Plamondon, "Automatic signature verification: the state of the art, 1989–1993," *International Journal of Pattern Recognition and Artificial Intelligence*, vol. 8, no. 3, pp. 643–660, 1994.
- [20] R. Plamondon and G. Lorette, "Automatic signature verification and writer identification—the state of the art," *Pattern Recognition*, vol. 22, no. 2, pp. 107–131, 1989.
- [21] R. Sabourin, R. Plamondon, and G. Lorette, "Off-line identification with handwritten signature images: survey and perspectives," in *Structured Document Image Analysis*, H. Baird, H. Bunke, and K. Yamamoto, Eds., pp. 219–234, Springer-Verlag, NY, USA, 1992.
- [22] J. Gupta and A. McCabe, "A review of dynamic handwritten signature verification," Tech. Rep., James Cook University, Australia, 1997.
- [23] R. N. Bracewell, *Two-Dimensional Imaging*, Prentice-Hall, Englewood Cliffs, NJ, USA, 1995.
- [24] L. R. Rabiner, "A tutorial on hidden Markov models and selected applications in speech recognition," *Proceedings of the IEEE*, vol. 77, no. 2, pp. 257–286, 1989.
- [25] J. R. Deller Jr., J. H. L. Hansen, and J. G. Proakis, *Discrete-Time Processing of Speech Signals*, IEEE Press, Piscataway, NJ, USA, 1999.
- [26] R. Auckenthaler, M. Carey, and H. Lloyd-Thomas, "Score normalization for text-independent speaker verification systems," *Digital Signal Processing*, vol. 10, no. 1, pp. 42–54, 2000.

**J. Coetzer** received his M.S. in applied mathematics from the University of the Free State, Bloemfontein, South Africa, in 1996. After an initial five years at the Department of Mathematics and Applied Mathematics, the University of the Free State, he joined the Department of Applied Mathematics, the University of Stellenbosch in mid 2002. His current research interests include pattern recognition and computer vision.



**B. M. Herbst** received his Ph.D. in applied mathematics from the University of the Free State, Bloemfontein, South Africa, in 1982. He visited the University of Dundee as a postdoc during 1983 and was a Visiting Associate Professor at Clarkson University, Potsdam, NY (from 1988 to 1989) and the University of Colorado, Boulder (from 1989 to 1990 and again during 1994). He joined the Department of Applied Mathematics at the University of Stellenbosch in 1998. His current research interests include scientific computation, pattern recognition, and computer vision.



**J. A. du Preez** received his Ph.D. in electronic engineering from the University of Stellenbosch, South Africa, in 1998, on the topic "Efficient high-order hidden Markov modelling." After an initial four years in the telecommunications sector, he joined the Department of Electrical and Electronic Engineering, the University of Stellenbosch in mid 1989. Active in the broader fields of signal processing and pattern recognition, his research focuses on biometrics and speech processing.

